TGR5 activation promotes stimulus-secretion coupling of pancreatic beta-cells via a PKA-dependent pathway

Jonas Maczewsky[1], Julia Kaiser[1], Anne Gresch[2], Felicia Gerst[3], Martina Düfer[2], Peter Krippeit-Drews[1], Gisela Drews[1]*

[1]Institute of Pharmacy, Department of Pharmacology, University of Tübingen, Auf der Morgenstelle 8, D-72076 Tübingen, Germany [2]Institute of Pharmaceutical and Medicinal Chemistry, Department of Pharmacology, University of Münster, Corrensstraße 48, D-48149 Münster, Germany [3]Institute for Diabetes Research and Metabolic Diseases of the Helmholtz Center Munich at the Eberhard Karls University of Tuebingen (IDM), Otfried-Müller-Straße 10, D-72076 Tübingen, University of Tübingen, Germany

Abbreviated title: TGR5 activation affects insulin secretion

Key terms: stimulus-secretion coupling, beta-cell, cytosolic Ca^{2+} concentration, exocytosis, TGR5, oleanolic acid, insulin secretion, protein kinase A

Word count: 4683

Number of figures: 9

**Corresponding author and person to whom reprint requests should be addressed*

Prof. Dr. Gisela Drews,

Institute of Pharmacy, Department of Pharmacology, University of Tübingen,

Auf der Morgenstelle 8, D-72076 Tübingen, Germany

Phone #49-7071-2977559

Fax #49-7071-295382 E-Mail: gisela.drews@uni-tuebingen.de

Diabetes Publish Ahead of Print, published online November 8, 2018

Abstract

The Takeda-G-protein-receptor-5 (TGR5) mediates physiological actions of bile acids. Since it was shown that TGR5 is expressed in pancreatic tissue, a direct TGR5 activation in beta-cells is currently postulated and discussed. The present study reveals that oleanolic acid (OLA) affects murine beta-cell function by TGR5 activation. Both, a $G_{\alpha s}$ inhibitor and an inhibitor of adenylyl cyclase (AC) prevented stimulating effects of OLA. Accordingly, OLA augmented the intracellular cAMP concentration. OLA and two well-established TGR5 agonists, RG239 and tauroursodeoxycholic acid (TUDCA), acutely promoted stimulus-secretion coupling (SSC). OLA reduced ATP-dependent K^+ (K_{ATP}) current and elevated current through Ca^{2+} channels. Accordingly, in mouse and human beta-cells TGR5 ligands increased the cytosolic Ca^{2+} concentration by stimulating Ca^{2+} influx. Higher OLA concentrations evoked a dual reaction, probably due to activation of a counter-regulating pathway. Protein kinase A (PKA) was identified as a downstream target of TGR5 activation. In contrast, inhibition of phospholipase C and phosphoinositide-3-kinase did not prevent stimulating effects of OLA. Involvement of exchange-protein-directly-activated-by-cAMP 2 (Epac2) or farnesoid-X-receptor (FXR) was ruled out by experiments with knockout mice. The proposed pathway was not influenced by local GLP-1 secretion from alpha-cells, shown by experiments with MIN6 cells, and a GLP-1 receptor antagonist. In summary, these data clearly demonstrate that activation of TGR5 in beta-cells stimulates insulin secretion via an AC/cAMP/PKA-dependent pathway which is supposed to interfere with SSC by affecting K_{ATP} and Ca^{2+} currents and thus membrane potential.

Introduction

In recent years, it became evident that the membrane protein Takeda-G-protein-receptor-5 (TGR5), also known as GPBA, MBAR or Gpbar1, plays an important role in energy and glucose metabolism (1; 2). TGR5 is present in several tissues and cell types including heart, spleen, intestine, macrophages, and pancreas (3; 4). The receptor is involved in physiological processes such as inflammation, gallbladder filling, gastrointestinal motility, and thermogenesis (1; 5-7). TGR5 stimulates secretion of glucagon-like-peptide-1 (GLP-1) from intestinal L-cells and thus regulates glucose metabolism (8-10). TGR5 activation leads to energy expenditure which in turn improves glucose homeostasis (9). Noteworthy, after vertical sleeve gastrectomy, TGR5 contributes to the beneficial effects of the surgery (11).

The endogenous ligands of the receptor are bile acids that potently regulate glucose homeostasis (3). For oleanolic acid (OLA), a triterpene isolated from *Olea europaea* which improves metabolic disorders and has anti-diabetic effects (12; 13), the situation is less clear. While OLA is proposed to be a TGR5 agonist in pancreatic islets by one study (4), another group excludes an increase in cAMP concentration by OLA normally observed downstream to TGR5 activation (14). In addition, direct effects of OLA on beta-cells through increased acetylcholine levels and the muscarinic M_3 receptor were reported (15).

Since it was discovered that TGR5 is present in pancreatic beta-cells, several *in vitro* studies described a direct effect of TGR5 on islet cell function (4; 16-18). First, Kumar et al. showed the stimulating effect of TGR5 agonists on insulin secretion in beta-cells by an increase of intracellular Ca^{2+} concentration ($[Ca^{2+}]_c$) due to Ca^{2+} release from intracellular stores (4). They postulated a pathway through cAMP, exchange-protein-directly-activated-by-cAMP (Epac) and phospholipase C (PLC) (4). In contrast, another study found that activation of TGR5 by the bile acid tauroursodeoxycholic acid (TUDCA) stimulates insulin secretion via protein kinase A (PKA) (16). This pathway was neither associated with changes in the activity

of ATP-dependent K^+ (K_{ATP}) channels nor with modified Ca^{2+} signals, but included an increase of cAMP, activation of PKA and phosphorylation of cAMP-response-element-binding-protein (CREB) (16). Both studies demonstrated TGR5 activation in clonal and murine beta-cells, respectively. However, the results point to completely different cAMP-mediated signaling pathways.

It cannot be ruled out that some effects of TGR5 agonists are mediated by the farnesoid-X-receptor (FXR). Some bile acids are able to rapidly activate a non-genomic FXR-dependent pathway in beta-cells (19). FXR and TGR5 are known to influence each other after ligand binding. However, the exact mechanism of this interaction has not been clarified yet (20).

Another *in vitro* study suggests that stimulating effects of TGR5 agonists in the pancreas are mainly due to GLP-1 released from alpha-cells which acts in a paracrine manner on beta-cells (18). Like GLP-1, activation of TGR5 improves mass and function of beta-cells in diabetic mouse models (21). Thus, TGR5 agonists might have a promising therapeutic profile (12).

Taken together, the potential of TGR5 to influence glucose metabolism was shown in several studies. However, the precise pathways and contribution of different islet cells and peripheral organs are still a matter of debate. Therefore, in the present study the direct effects of OLA and two well-known TGR5 agonists on beta-cell stimulus-secretion coupling (SSC) were investigated.

Research Design and Methods

Cell and islet preparation. Details are described in (22). In brief, mouse islets were isolated by injecting collagenase (0.5-1 mg/ml) into the pancreas and by handpicking after digestion at 37°C. Male and female wild type C57Bl/6 (WT) mice were used in equal shares. FXR knockout ($FXR^{-/-}$) mice and Epac2 knockout ($Epac2^{-/-}$) mice are all on a C57Bl/6 background and were housed under same conditions. Mice were bred in the animal facility of the Department of Pharmacology at the University of Tübingen. Principles of laboratory animal care (NIH publication no. 85-23, revised 1985) and German laws were followed. Human islets were provided by the JDRF award 31-2008-416 (ECIT Islet for Basic Research Program) from Islet Transplantation Centre (Milan). Mouse and human islets were dispersed to single cells and cell clusters, respectively, by trypsin treatment.

Solutions and chemicals. Recordings of $[Ca^{2+}]_c$ were performed with a bath solution which contained (in mM): 140 NaCl, 5 KCl, 1.2 $MgCl_2$, 2.5 $CaCl_2$, glucose as indicated, 10 HEPES, pH 7.4 adjusted with NaOH. The same bath solution was used for patch-clamp measurements to record K_{ATP} current and membrane potential (V_m) in the perforated-patch configuration. For Ca^{2+} current measurements in the perforated-patch configuration bath solution consisted of (in mM): 115 NaCl, 1.2 $MgCl_2$, 10 $CaCl_2$, 10 tetraethylammonium chloride (TEA), 10 HEPES, 15 glucose, 0.1 tolbutamide, pH 7.4 adjusted with NaOH. Krebs-Ringer-HEPES solution (KRH) for insulin secretion was composed of (in mM): 120 NaCl, 4.7 KCl, 1.1 $MgCl_2$, 2.5 $CaCl_2$, glucose as indicated, 10 HEPES, 0.5 % bovine serum albumin (BSA) and pH 7.4 adjusted with NaOH. Pipette solution for cell-attached K_{ATP} current and V_m recordings consisted of (in mM): 10 KCl, 10 NaCl, 70 K_2SO_4, 4 $MgCl_2$, 2 $CaCl_2$, 10 EGTA, 20 HEPES, 0.27 amphotericin B, pH adjusted to 7.15 with KOH. To determine the Ca^{2+} currents, pipette solution was composed of (in mM): 10 KCl, 10 NaCl, 7 $MgCl_2$, 70 Cs_2SO_4, 10 HEPES, 0.27 amphotericin B, pH adjusted to 7.15 with NaOH. Murine islet cell clusters and islets were

cultured in RPMI 1640 (11.1 mM glucose) enriched with 10 % fetal calf serum (FCS) and 1 % penicillin/streptomycin. MIN6 cells were incubated in DMEM containing 22.2 mM glucose, 15 % FCS and 1 % penicillin/streptomycin. Human islets were kept in CMRL medium with 5.5 mM glucose.

OLA and NF449 were obtained from Biomol (Hamburg, Germany). Fura-2-AM was purchased from Biotrend (Köln, Germany). Edelfosine and myristoylated protein kinase A inhibitor 14-22 amide (Myr-PKI) were from Tocris (Wiesbaden, Germany). RPMI 1640 medium, FCS, penicillin/streptomycin and trypsin were from Invitrogen (Karlsruhe, Germany). DMEM medium was from Biozym (Hessisch Oldendorf, Germany). TUDCA was obtained from Merck (Darmstadt, Germany) and exendin 9-39 amide (exendin 9-39) from Bachem (Bubendorf, Switzerland). The cAMP ELISA Kit was from Cayman Chemical, Ann Arbor, USA. All other chemicals were purchased from Sigma (Deisenhofen, Germany) or Merck (Darmstadt, Germany) in the purest form available.

Measurement of $[Ca^{2+}]_c$. Details are described in (22). In brief, cells were loaded with 5 µM Fura-2-AM for 35 min at 37°C. Fluorescence was excited at 340 and 380 nm and emission filtered (LP515) and measured by a digital camera. $[Ca^{2+}]_c$ was calculated according to an *in vitro* calibration. The mean $[Ca^{2+}]_c$ over 10 minutes at the end of each interval was calculated to compare $[Ca^{2+}]_c$ under different experimental conditions.

Patch-clamp measurements. Patch pipettes were pulled from borosilicate glass capillaries (Harvard Apparatus, March-Hugstetten, Germany). Ionic currents and V_m were recorded with an EPC-9 patch-clamp amplifier using Patchmaster software (HEKA, Lambrecht, Germany). To determine the K_{ATP} current, pulses of 300 ms were performed every 15 s from the holding potential at -70 mV to -60 mV and to -80 mV, the equivalence potential without any current. The amplitude of currents elicited by voltage steps from the holding potential to -60 mV were taken for evaluation. Data of the last 3 pulses in each interval were averaged and normalized

to control condition. Ca^{2+} currents were triggered by 100 ms steps from -70 mV to 0 mV. K^+ currents were blocked by TEA, K^+ free bath solution, and the K_{ATP} channel antagonist tolbutamide. The maximum Ca^{2+} current was analyzed. For statistics the currents of 3 succeeding pulses for each measuring point were averaged and data were normalized to control condition. V_m measurements were evaluated by determination of the plateau potential (from which spikes start) and spike frequency during a 1 min interval after achievement of the maximum OLA effect (min 4 to 7 after application). In experiments with KT5720 plateau potential and spike frequency were estimated during 1 min before OLA application and at min 5 to 6 after OLA addition.

Insulin secretion. Details for steady-state incubations are described in (23). Briefly, batches of 5 islets in triplicate were incubated in 1 ml KRH for 1 h at 37°C under conditions as indicated. For perifusion experiments bath chambers were equipped with 50 islets and perifused with KRH under conditions as indicated at a rate of 0.7 ml/min at 37°C. Eluate samples were taken every 2 min. MIN6 cells were incubated for 1 h at 37°C under conditions as indicated. To determine the first phase of insulin secretion, AUC was calculated between min 6 (start of increase) and 21 after the switch to 15 mM glucose.

Insulin was determined by radioimmunoassay (RIA) (Merck Millipore, Darmstadt, Germany). Results are presented as the secreted insulin per islet in a specific time. In addition, for MIN6 cells secreted insulin was normalized to the total insulin content and high glucose control condition.

Measurement of cAMP. Batches of 100 islets were incubated in 2 ml KRH for 1 h at 37°C under conditions as indicated. Thereafter, buffer was removed and islets were lysed in 0.1 mol/l HCl. Supernatant was used for measuring cAMP by ELISA according to the manufacturer´s protocol.

Statistics. Each series of experiments was performed with islets or islet cells from at least 3 different mice. Means ± SEM are given for the indicated number of experiments (cell clusters or islets). Statistical significance of differences was assessed by a paired Student´s t test. Multiple comparisons were made by repeated ANOVA followed by Student-Newman-Keuls test. P values ≤ 0.05 were considered significant.

Results

Effect of OLA on $[Ca^{2+}]_c$ and insulin secretion

The triterpene OLA, extracted from olive leaves, is a powerful modulator of glucose homeostasis (12; 13). However, it is not clear by which receptors and downstream pathways OLA interferes with SSC. To evaluate whether OLA affects beta-cell function, its effects on $[Ca^{2+}]_c$ and insulin secretion in isolated beta-cells and islets, respectively, were investigated. In the presence of 15 mM glucose $[Ca^{2+}]_c$ oscillated. OLA increased mean $[Ca^{2+}]_c$ in WT mouse beta-cells (Fig. 1A-D). Fig. 1E,F reveals that OLA also augmented $[Ca^{2+}]_c$ in human beta-cells. To evaluate how this change in $[Ca^{2+}]_c$ affects insulin secretion, perifusion experiments with islets of WT mice were performed. Switching from a low to a stimulating glucose concentration evoked the typical biphasic pattern. A first peak secretion (1st phase) is followed by consistent release at a lower level (2nd phase). Addition of 1 µM OLA to the 2nd phase slightly augmented insulin secretion (Fig. 2A). The mean insulin secretion rate for 10 min increased from 22±3 pg insulin/(min∗islet) under control condition to 24±3 pg insulin/(min∗islet) (Fig. 2B). In addition to this small, yet significant effect, the first phase was analyzed in the presence of 1 µM OLA (Fig. 2C). The mean insulin secretion (AUC) during the first 15 min of the 1st phase of insulin secretion under high glucose condition was clearly augmented in the presence of 1 µM OLA (37±6 pg insulin/(min∗islet)) in comparison to control condition without OLA (27±3 pg insulin/(min∗islet)) (Fig. 2D).

Steady-state insulin secretion comprises both phases of insulin secretion. Application of 1 µM and 10 µM OLA augmented insulin secretion in the presence of 15 mM glucose to 147±11 % and to 145±16 %, respectively (Fig. 2E). 0.1 µM OLA was without effect (113±5 %).

The glucose dependency of the drug effect was tested in the presence of 1 µM OLA. OLA did not affect basal insulin secretion at 3 mM glucose but increased it above the threshold

concentration for the initiation of insulin secretion (8 mM) and at higher glucose concentrations (Fig. 2F).

Dependence of OLA-mediated effects on $G_{\alpha s}$ and FXR

OLA structurally resembles bile acids. Since acute effects of bile acids in beta-cells can be mediated by FXR (19), a possible interaction of the TGR5 agonist with this receptor was investigated. In beta-cells of $FXR^{-/-}$ mice, 1 µM OLA increased mean $[Ca^{2+}]_c$ similarly to the effect in WT mice (Fig. 3A,B). Accordingly, 1 µM OLA enhanced insulin secretion from islets of $FXR^{-/-}$ mice (Fig. 3C).

Since the TGR5 is G_s-coupled, the influence of NF449, an inhibitor of the $G_{\alpha s}$ subunit, on TGR5 activation was investigated to test for this pathway. 10 µM NF449 did not affect insulin secretion but completely blocked the stimulating effect evoked by OLA in islets of WT mice (Fig. 3D).

Confirmation of the influence of TGR5 activation on beta-cell function by two other TGR5 agonists

The synthetic TGR5 agonist RG239 (1 µM) increased mean $[Ca^{2+}]_c$ (Fig. 4A,B) and insulin secretion (Fig. 4C). TUDCA (50 µM), another TGR5 ligand with bile acid structure, provided very similar results on mean $[Ca^{2+}]_c$ (Fig. 4D,E) and insulin secretion (Fig. 4F) emphasizing the significance of TGR5 for beta-cell function.

Effects of OLA on K_{ATP} and Ca^{2+} channel currents

In the well accepted model of SSC in beta-cells increased $[Ca^{2+}]_c$ can result from Ca^{2+} influx due to closure of K_{ATP} channels with subsequent opening of voltage-dependent Ca^{2+} channels (VDCCs) or to opening of VDCCs. Activity of both channels can be affected by protein kinases (24-26). Patch-clamp measurements showed an acute effect on K_{ATP} current after

OLA administration. In recordings with the perforated-patch configuration, 1 μM OLA reduced the K_{ATP} current measured in WT beta-cells to 54±3 % (12.2±1.2 pA) of the control current (100 %, 22.8±2.4 pA) in the presence of 0.5 mM glucose (Fig. 5A,B). The effect was dose-dependent. The inhibitory effect of 10 μM OLA on the K_{ATP} current showed a faster onset of action and reduced the current to 22±2 % (7.3±1.3 pA) of the control level (100 %, 32.9±5.3 pA) (Fig. 5C,D). The currents were identified as K_{ATP} channel currents by using the K_{ATP} opener diazoxide at the end of each measurement.

As mentioned above, phosphorylation may influence VDCCs. The peak Ca^{2+} current, measured in the perforated-patch configuration, was increased to 118±2 % (70.8±9.9 pA) and 122±3 % (73.2±10.4 pA) after 2 and 4 minutes of 1 μM OLA administration, respectively, compared to control condition (100 %, 60.5±8.8 pA) (Fig. 5E,F). At the higher OLA concentration of 10 μM peak Ca^{2+} current was augmented after 2 min of drug application but strongly inhibited after 8 min (Fig. 6A,B). 10 μM OLA also affected 2nd phase insulin secretion in a biphasic manner (Fig. 6C,D). Evidently, higher concentrations of OLA induce a counter-regulating pathway. This observation could explain why 10 μM OLA were not more effective than 1 μM on steady-state insulin secretion (Fig. 2E).

At a first glance it may seem astonishing that a clear dual effect of 10 μM OLA on $[Ca^{2+}]_c$ is missing (Fig 1C). However, despite the strong inhibition of Ca^{2+} currents by 10 μM OLA (Fig. 6), substantial Ca^{2+} influx may remain. First, K_{ATP} current is also markedly reduced by 10 μM OLA (Fig. 5) prolonging the burst time during which Ca^{2+} channels open (see Fig. 1C transition from oscillations to a plateau in the presence of 10 μM OLA). Second, inhibition of K_{ATP} current will further depolarize the cells leading to increased opening of Ca^{2+}- and voltage-dependent BK channels resulting in enhanced Ca^{2+} influx during a single AP. This assumption is based on the observation that inhibition of BK channels decreases Ca^{2+} influx (27). Nevertheless, the transient effect of 10 μM OLA on $[Ca^{2+}]_c$ can be detected by

evaluating maximum Ca^{2+} concentration. In the experiments presented in Fig. 1, maximum Ca^{2+} increased from 831±45 nM (n=26) in the presence of 15 mM glucose to 1167±75 nM (n=26, $P \leq 0.001$) after application of 10 µM OLA if the usual evaluation procedure (last 10 min of the application interval) is used. However, it amounts to 874±68 nM if only the last 2 min of OLA application are evaluated (n=26, n.s. *vs*. 15 mM glucose). This shows a clear reduction of maximum Ca^{2+} concentration over time during OLA application.

K_{ATP} and L-type Ca^{2+} channel currents are two key determinants of the membrane potential of beta-cells. Thus, the observed effects on the ion channels should result in changes of the plasma membrane potential V_m. Fig. 6E-G reveals that OLA depolarized V_m and increased the number of action potentials. The described effects were completely suppressed in the presence of the established PKA inhibitor KT5720 (Fig. 6H-K) pointing to an involvement of this kinase in the OLA-evoked changes in channel activities.

Influence of OLA-evoked TGR5 activation on adenylyl cyclase and Epac2

The TGR5 belongs to the group of G_s-coupled receptors. The $G_{\alpha s}$ subunit is known to activate adenylyl cyclase (AC), which leads to cAMP production (3). To verify this pathway for OLA, the AC inhibitor 2´5´-dideoxyadenosine (DDA) was used in insulin secretion experiments. Remarkably, DDA (100 µM) alone had a stimulating effect on insulin secretion (Fig. 7A). In the presence of DDA OLA did no longer stimulate insulin secretion but rather reduced it. Furthermore, OLA (1 µM) increased the intracellular cAMP concentration by about 23 % in 5 out of 6 experiments (Fig. 7B). In one experiment we observed a paradoxical decrease of ~10 %.

Since Epac is one of the postulated targets of cAMP, islets and beta-cells of $Epac2^{-/-}$ mice were used to investigate an involvement of this protein in the OLA-activated pathway. Epac2 is the most abundant isoform in beta-cells (28). $[Ca^{2+}]_c$ measurements did not reveal any

influence of Epac2 on the stimulating effect of 1 μM OLA (Fig. 7C). Moreover, the stimulating effects of OLA and RG239 on insulin secretion were still present in islets from Epac2$^{-/-}$ mice (Fig. 7D).

Involvement of PKA in the signaling cascade downstream TGR5 activation

To further evaluate a possible participation of PKA in the TGR5 signaling pathway, the established PKA inhibitors Myr-PKI and KT5720 were tested on OLA-evoked insulin secretion. Myr-PKI itself increased insulin secretion while KT5720 alone was without a significant effect compared to the respective control conditions in WT islets. Both inhibitors suppressed the stimulatory effect of 1 μM OLA in the presence of 15 mM glucose (Fig. 8A,B). OLA even inhibited insulin secretion under these conditions. Since PLC is supposed to be involved in the TGR5 pathway by Kumar et al. (4), the PLC inhibitor edelfosine was applied. In contrast to PKA inhibitors, edelfosine (10 μM) did not prevent the stimulation evoked by 1 μM OLA (Fig. 8C, same controls as in A).

Phosphoinositide-3-kinase (PI3K) is also proposed to be involved in the signaling pathway downstream to TGR5 activation. The PI3K inhibitor wortmannin did not prevent but even amplified the OLA effect on insulin secretion (Fig. 8D, same controls as in B). Edelfosine or wortmannin alone did not change insulin secretion induced by 15 mM glucose.

Alpha-cells and GLP-1 are not involved in effects of OLA in beta-cells

Alpha-cells are capable to secrete GLP-1 and activation of TGR5 is known to increase GLP-1 production and secretion (18). To exclude that GLP-1 contributes to the OLA-evoked effects in beta-cells, the GLP-1 receptor antagonist exendin 9-39 was used in secretion experiments. Exendin 9-39 did not prevent the stimulating effect of 1 μM OLA on insulin secretion (Fig. 9A). The potency of the inhibitor exendin 9-39 at the GLP-1 receptor was proved by the fact that the stimulation of 50 nM GLP-1 was completely blocked by the antagonist (Fig. 9B, same

controls as in A). Notably, 100 nM exendin 9-39 alone did not significantly alter the amount of secreted insulin. To circumvent a possible influence of alpha-cells, the beta-cell line MIN6 was used to perform insulin secretion experiments. Insulin secretion of MIN6 cells was dependent on the glucose concentration (insulin levels reached 26.6±2.9 % at low glucose concentration compared to a stimulatory concentration of 15 mM glucose). Application of 1 µM and 10 µM OLA significantly increased insulin secretion to 111.5±3.0 % and 121.4±7.8 %, respectively, compared to 15 mM glucose alone (Fig. 9C). These experiments support the assumption that the TGR5 agonist OLA acts directly on beta-cells.

Discussion

OLA directly stimulates beta-cells by binding to the TGR5

During the last decades, it became evident that TGR5 agonists are important contributors to the regulation of glucose metabolism. Several studies have shown reduction of blood glucose concentration and improvement of the energy expenditure by TGR5 agonists, e.g. (9; 12; 29). TGR5 activation in L-cells crucially affects GLP-1 secretion (30). Here, we identify OLA as a TGR5 agonist of beta-cells and show a stimulating effect of OLA and two other TGR5 agonists, RG239 and TUDCA, on islets of Langerhans *in vitro* excluding factors like GLP-1 secreted from L-cells. TGR5 activation concurrently affects several parameters of stimulus-secretion coupling (SSC) including current through K_{ATP} channels and voltage-dependent Ca^{2+} channels and, as a result, V_m. Changes in the activity of these channels are followed by enhanced $[Ca^{2+}]_c$ and insulin secretion. Kumar and colleagues also demonstrated a direct effect on isolated beta-cells after TGR5 agonist administration (4). In their study OLA leads to enhanced glucose-induced insulin secretion, however, an increase in $[Ca^{2+}]_c$ is only shown at substimulatory glucose concentration and is attributed to release from intracellular Ca^{2+} stores. This effect cannot account for increased insulin secretion after stimulation of beta-cells

with glucose. In contrast, our data clearly show that enhanced Ca^{2+} influx contributes to increased $[Ca^{2+}]_c$ after TGR5 activation at stimulatory glucose concentration and not at basal one.

In alpha-cells, alternative splicing of proglucagon enables synthesis and secretion of GLP-1 (17). Kumar and co-workers observed an increased GLP-1 secretion from pancreatic alpha-cells after TGR5 activation (18). They suggest that this is mediated via the cAMP/Epac/PLC-dependent pathway. Moreover, synthesis of GLP-1 in alpha-cells was stimulated by the cAMP/PKA/pCREB cascade. The authors provide evidence that this pathway is activated by hyperglycemia (18). To examine a possible GLP-1-mediated stimulation of insulin secretion after TGR5 activation under physiological conditions we blocked the GLP-1 receptor by the antagonist exendin 9-39 (31). Since exendin 9-39 did not prevent the effect of OLA we conclude that OLA stimulates insulin secretion independent of GLP-1 receptor activation. Kumar et al. performed a similar experiment with human islets, but with a higher concentration of exendin 9-39 and after culturing the islets in the presence of 25 mM glucose for 7 days (18). They claim that in this glucotoxic model exendin 9-39 reduces the effect of the TGR5 agonist INT-777, however this reduction is marginal and insulin release is still ~ 2fold higher than the effect of glucose alone. Our view that the effects of TGR5 agonists are not mediated by GLP-1 released by alpha-cells is further supported by the observation that OLA increased insulin secretion of MIN6 cells. The MIN6 cell line solely consists of clonal beta-cells and an effect of locally secreted GLP-1 from other cell types can be ruled out (32).

TGR5 agonists are structural analogs of bile acids, the endogenous activators of TGR5. Bile acids acutely affect additional targets regulating glucose metabolism, particularly the FXR (19; 33). In beta-cells, Vettorazzi and colleagues found that TUDCA activates a TGR5-dependent pathway and suggested that FXR is not involved (16). In the present study, the involvement of FXR was excluded due to experiments with a $FXR^{-/-}$ mouse model. Teodoro

and co-workers also showed a stimulating effect of OLA on insulin secretion but excluded increased cAMP concentration and thus involvement of the TGR5 as explanation for this observation (14). In contrast, our results with inhibitors of the $G_{\alpha s}$ subunit and the AC clearly indicate a TGR5-dependent pathway for OLA.

OLA acts via a cAMP/PKA-dependent pathway

The TGR5/$G_{\alpha s}$/AC pathway results in increased cAMP concentrations (5; 34). This fits well to the OLA-induced increase of the cAMP concentration and the loss of efficacy of OLA after inhibition of AC in our experiments. Enhanced cAMP levels are known to activate PKA and/or Epac, which is also described for beta-cells (4; 16; 30). Kumar et al. exclude any influence of OLA on PKA in beta-cells but describe a pathway via Epac, followed by PLC activation which leads to enhanced insulin secretion (4). This suggestion is based on a single series of secretion experiments with MIN6 cells and the high concentration of 50 µM OLA (4). Moreover, Kumar and colleagues blocked the effect of 50 µM OLA with the PLC antagonist U73122 (4). However, the used concentration of U73122 can exert unspecific effects, such as modulation of TRPM3/4 channels as well as stimulation of IP_3 synthesis and mobilization of Ca^{2+} from intracellular stores (35-37).

To clarify the discrepancy to our results, we used an Epac2$^{-/-}$ mouse model. Epac2 is more abundant compared to Epac1 and is an important target of cAMP in beta-cells (28; 30). Since TGR5 agonists effectively enhanced $[Ca^{2+}]_c$ and insulin secretion in beta-cells and islets of Epac2$^{-/-}$ mice, an involvement of Epac2 seems to be unlikely. Nevertheless, a possible influence of Epac1 should be considered. Likewise, PLC blockade by edelfosine was unable to suppress the OLA effect on insulin secretion also speaking against an involvement of the Epac/PLC pathway after TGR5 activation.

PI3K has been identified as another downstream target of Epac in processes like angiogenesis or stem cell differentiation (38; 39). The PI3K inhibitor wortmannin revealed that PI3K seems not to be involved in stimulating effects of OLA.

We identified PKA as the downstream kinase in the TGR5/cAMP pathway. OLA completely lost the stimulating effect on insulin secretion after PKA inhibition with two different PKA inhibitors, Myr-PKI and KT5720. This is supported by findings of Vettorazzi and co-workers who showed that the TGR5 agonist TUDCA was ineffective in stimulating insulin secretion in the presence of the PKA inhibitor H89 (16). Worth mentioning, the link between cAMP and PKA is clearly demonstrated for the GLP-1 pathway in beta-cells (40; 41).

The puzzling observation that inhibition of AC or PKA leads to stimulation of insulin secretion may be due to a crosstalk between cAMP and cGMP as described for other organs (42; 43) especially activation of a cGMP-specific PDE by PKA (44; 45). Inhibition of PKA would thus increase cGMP concentration leading to PKG-dependent closure of K_{ATP} channels (46). Inhibition of the AC by DDA would also reduce PKA activity with similar consequences at least for the cGMP/PKG/K_{ATP} channel signaling pathway. Remarkably, during inhibition of the AC/cAMP/PKA pathway OLA is not without effect but exerts inhibition of insulin secretion. This is most likely due to the biphasic effect of OLA. Apparently, after inhibition of the stimulatory pathway the inhibitory one that is PKA-independent prevails.

K_{ATP} and VDCCs mediate stimulating effects of OLA

Although having results in favor of the PKA pathway, Vettorazzi and colleagues did not find any changes in K_{ATP} channel activity or $[Ca^{2+}]_c$ after TGR5 activation in beta-cells (16). In our experiments, OLA caused both, a distinct reduction of the K_{ATP} current and an increase in Ca^{2+} current, probably due to phosphorylation of both channel proteins by PKA. After PKA activation, K_{ATP} channel activity is reduced resulting in membrane depolarization and

enhanced insulin secretion (24). Suitably, OLA-evoked changes in V_m, which are a result of the effects on the channels, are suppressed by the PKA inhibitor KT5720.

The VDCC in pancreatic islet cells is a possible target to control insulin secretion (47). Phosphorylation of VDCCs could affect channel activity thus increasing the Ca^{2+} current (25; 26). Worth mentioning, the effect of OLA on VDCCs is not secondary to inhibition of K_{ATP} channels since the latter ones were not functional under the relevant experimental conditions. Thus, K_{ATP} channel closure and VDCC activation together cause increased $[Ca^{2+}]_c$ followed by enhanced insulin secretion. Since OLA increases $[Ca^{2+}]_c$ in human beta-cells, it is assumed that the suggested mechanism is also relevant for human beta-cells. The proposed direct interaction of PKA with ion channels would result in a rapid effect after TGR5 activation. However, we cannot exclude that other mechanisms besides changes in ion channel activity contribute to the stimulatory effects of TGR5 activation. The cAMP-PKA pathway can directly increase granule exocytosis by enhancing the sensitivity of the exocytotic machinery to Ca^{2+} (48; 49). Two other groups postulated modified protein synthesis by PKA-mediated phosphorylation of CREB (16; 18). Such a mechanism is inconsistent with the rapid effects on SSC starting within seconds. However, protein synthesis may account for effects on exocytosis after prolonged exposure to TGR5 agonists (14; 16; 18).

In summary, we clearly demonstrated that OLA affects beta-cell SSC via TGR5 activation and that TGR5 agonists directly stimulate beta-cells to secrete insulin. The data suggest a pathway including AC activation, PKA, closure of K_{ATP} and opening of Ca^{2+} channels and increased Ca^{2+} influx. This insulinotropic effect opens new possibilities for pharmaceutical applications of drugs like OLA.

Acknowledgments

We are grateful to Isolde Breuning for her excellent and skillful technical assistance. The authors thank Jelena Sikimic for performing some of the experiments with human islet cells and Friederike Anna Steudel and Nia Blackwell for careful and excellent revision of the manuscript. This work was supported by a grant from the DFG (G.D.).

Author´s contribution: J.M. researched data, wrote and edited the manuscript; J.K., A.G. and F.G. researched data; M.D. and P.K.-D. contributed to discussion and study design and edited the manuscript; G.D. designed the study, wrote and edited the manuscript and contributed to discussion.

G.D. is the guarantor of this work and, as such, had full access to all the data in the study and takes responsibility for the integrity of the data and the accuracy of the data analysis.

Disclosure Summary: The authors have nothing to disclose.

References

1. Watanabe M, Houten SM, Mataki C, Christoffolete MA, Kim BW, Sato H, Messaddeq N, Harney JW, Ezaki O, Kodama T, Schoonjans K, Bianco AC, Auwerx J: Bile acids induce energy expenditure by promoting intracellular thyroid hormone activation. Nature 2006;439:484-489
2. Katsuma S, Hirasawa A, Tsujimoto G: Bile acids promote glucagon-like peptide-1 secretion through TGR5 in a murine enteroendocrine cell line STC-1. Biochem Biophys Res Commun 2005;329:386-390
3. Kawamata Y, Fujii R, Hosoya M, Harada M, Yoshida H, Miwa M, Fukusumi S, Habata Y, Itoh T, Shintani Y, Hinuma S, Fujisawa Y, Fujino M: A G protein-coupled receptor responsive to bile acids. J Biol Chem 2003;278:9435-9440
4. Kumar DP, Rajagopal S, Mahavadi S, Mirshahi F, Grider JR, Murthy KS, Sanyal AJ: Activation of transmembrane bile acid receptor TGR5 stimulates insulin secretion in pancreatic beta cells. Biochem Biophys Res Commun 2012;427:600-605
5. Pols TW, Nomura M, Harach T, Lo Sasso G, Oosterveer MH, Thomas C, Rizzo G, Gioiello A, Adorini L, Pellicciari R, Auwerx J, Schoonjans K: TGR5 activation inhibits atherosclerosis by reducing macrophage inflammation and lipid loading. Cell Metab 2011;14:747-757
6. Vors C, Pineau G, Drai J, Meugnier E, Pesenti S, Laville M, Laugerette F, Malpuech-Brugere C, Vidal H, Michalski MC: Postprandial Endotoxemia Linked With Chylomicrons and Lipopolysaccharides Handling in Obese Versus Lean Men: A Lipid Dose-Effect Trial. The Journal of clinical endocrinology and metabolism 2015;100:3427-3435
7. Li T, Holmstrom SR, Kir S, Umetani M, Schmidt DR, Kliewer SA, Mangelsdorf DJ: The G protein-coupled bile acid receptor, TGR5, stimulates gallbladder filling. Mol Endocrinol 2011;25:1066-1071
8. Harach T, Pols TW, Nomura M, Maida A, Watanabe M, Auwerx J, Schoonjans K: TGR5 potentiates GLP-1 secretion in response to anionic exchange resins. Sci Rep 2012;2:430
9. Thomas C, Gioiello A, Noriega L, Strehle A, Oury J, Rizzo G, Macchiarulo A, Yamamoto H, Mataki C, Pruzanski M, Pellicciari R, Auwerx J, Schoonjans K: TGR5-mediated bile acid sensing controls glucose homeostasis. Cell Metab 2009;10:167-177
10. Parker HE, Wallis K, le Roux CW, Wong KY, Reimann F, Gribble FM: Molecular mechanisms underlying bile acid-stimulated glucagon-like peptide-1 secretion. Br J Pharmacol 2012;165:414-423
11. McGavigan AK, Garibay D, Henseler ZM, Chen J, Bettaieb A, Haj FG, Ley RE, Chouinard ML, Cummings BP: TGR5 contributes to glucoregulatory improvements after vertical sleeve gastrectomy in mice. Gut 2017;66:226-234
12. Castellano JM, Guinda A, Delgado T, Rada M, Cayuela JA: Biochemical basis of the antidiabetic activity of oleanolic acid and related pentacyclic triterpenes. Diabetes 2013;62:1791-1799
13. Sato H, Genet C, Strehle A, Thomas C, Lobstein A, Wagner A, Mioskowski C, Auwerx J, Saladin R: Anti-hyperglycemic activity of a TGR5 agonist isolated from Olea europaea. Biochem Biophys Res Commun 2007;362:793-798
14. Teodoro T, Zhang L, Alexander T, Yue J, Vranic M, Volchuk A: Oleanolic acid enhances insulin secretion in pancreatic beta-cells. FEBS Lett 2008;582:1375-1380
15. Hsu JH, Wu YC, Liu IM, Cheng JT: Release of acetylcholine to raise insulin secretion in Wistar rats by oleanolic acid, one of the active principles contained in Cornus officinalis. Neurosci Lett 2006;404:112-116
16. Vettorazzi JF, Ribeiro RA, Borck PC, Branco RC, Soriano S, Merino B, Boschero AC, Nadal A, Quesada I, Carneiro EM: The bile acid TUDCA increases glucose-induced insulin secretion via the cAMP/PKA pathway in pancreatic beta cells. Metabolism 2016;65:54-63

17. Whalley NM, Pritchard LE, Smith DM, White A: Processing of proglucagon to GLP-1 in pancreatic alpha-cells: is this a paracrine mechanism enabling GLP-1 to act on beta-cells? J Endocrinol 2011;211:99-106
18. Kumar DP, Asgharpour A, Mirshahi F, Park SH, Liu S, Imai Y, Nadler JL, Grider JR, Murthy KS, Sanyal AJ: Activation of transmembrane bile acid receptor TGR5 modulates pancreatic islet alpha cells to promote glucose homeostasis. J Biol Chem 2016;291:6626-6640
19. Düfer M, Hörth K, Wagner R, Schittenhelm B, Prowald S, Wagner TF, Oberwinkler J, Lukowski R, Gonzalez FJ, Krippeit-Drews P, Drews G: Bile acids acutely stimulate insulin secretion of mouse beta-cells via farnesoid X receptor activation and K_{ATP} channel inhibition. Diabetes 2012;61:1479-1489
20. Pathak P, Liu H, Boehme S, Xie C, Krausz KW, Gonzalez F, Chiang JYL: Farnesoid X receptor induces Takeda G-protein receptor 5 cross-talk to regulate bile acid synthesis and hepatic metabolism. J Biol Chem 2017;292:11055-11069
21. Zheng C, Zhou W, Wang T, You P, Zhao Y, Yang Y, Wang X, Luo J, Chen Y, Liu M, Chen H: A novel TGR5 activator WB403 promotes GLP-1 secretion and preserves pancreatic beta-cells in type 2 diabetic mice. PLoS One 2015;10:e0134051
22. Gier B, Krippeit-Drews P, Sheiko T, Aguilar-Bryan L, Bryan J, Düfer M, Drews G: Suppression of K_{ATP} channel activity protects murine pancreatic beta cells against oxidative stress. J Clin Invest 2009;119:3246-3256
23. Maczewsky J, Sikimic J, Bauer C, Krippeit-Drews P, Wolke C, Lendeckel U, Barthlen W, Drews G: The LXR ligand T0901317 acutely inhibits insulin secretion by affecting mitochondrial metabolism. Endocrinology 2017;
24. Light PE, Manning Fox JE, Riedel MJ, Wheeler MB: Glucagon-like peptide-1 inhibits pancreatic ATP-sensitive potassium channels via a protein kinase A- and ADP-dependent mechanism. Mol Endocrinol 2002;16:2135-2144
25. Leiser M, Fleischer N: cAMP-dependent phosphorylation of the cardiac-type alpha 1 subunit of the voltage-dependent Ca2+ channel in a murine pancreatic beta-cell line. Diabetes 1996;45:1412-1418
26. Fuller MD, Fu Y, Scheuer T, Catterall WA: Differential regulation of CaV1.2 channels by cAMP-dependent protein kinase bound to A-kinase anchoring proteins 15 and 79/150. J Gen Physiol 2014;143:315-324
27. Düfer M, Neye Y, Hörth K, Krippeit-Drews P, Hennige A, Widmer H, McClafferty H, Shipston MJ, Häring HU, Ruth P, Drews G: BK channels affect glucose homeostasis and cell viability of murine pancreatic beta cells. Diabetologia 2011;54:423-432
28. Sugawara K, Shibasaki T, Takahashi H, Seino S: Structure and functional roles of Epac2 (Rapgef4). Gene 2016;575:577-583
29. Thomas C, Pellicciari R, Pruzanski M, Auwerx J, Schoonjans K: Targeting bile-acid signalling for metabolic diseases. Nat Rev Drug Discov 2008;7:678-693
30. Dzhura I, Chepurny OG, Leech CA, Roe MW, Dzhura E, Xu X, Lu Y, Schwede F, Genieser HG, Smrcka AV, Holz GG: Phospholipase C-epsilon links Epac2 activation to the potentiation of glucose-stimulated insulin secretion from mouse islets of Langerhans. Islets 2011;3:121-128
31. Thorens B, Porret A, Buhler L, Deng SP, Morel P, Widmann C: Cloning and functional expression of the human islet GLP-1 receptor. Demonstration that exendin-4 is an agonist and exendin-(9-39) an antagonist of the receptor. Diabetes 1993;42:1678-1682
32. Miyazaki J, Araki K, Yamato E, Ikegami H, Asano T, Shibasaki Y, Oka Y, Yamamura K: Establishment of a pancreatic beta cell line that retains glucose-inducible insulin secretion: special reference to expression of glucose transporter isoforms. Endocrinology 1990;127:126-132
33. Schittenhelm B, Wagner R, Kähny V, Peter A, Krippeit-Drews P, Düfer M, Drews G: Role of FXR in beta-Cells of Lean and Obese Mice. Endocrinology 2015;156:1263-1271

34. Bala V, Rajagopal S, Kumar DP, Nalli AD, Mahavadi S, Sanyal AJ, Grider JR, Murthy KS: Release of GLP-1 and PYY in response to the activation of G protein-coupled bile acid receptor TGR5 is mediated by Epac/PLC-epsilon pathway and modulated by endogenous H2S. Front Physiol 2014;5:420
35. Leitner MG, Michel N, Behrendt M, Dierich M, Dembla S, Wilke BU, Konrad M, Lindner M, Oberwinkler J, Oliver D: Direct modulation of TRPM4 and TRPM3 channels by the phospholipase C inhibitor U73122. Br J Pharmacol 2016;173:2555-2569
36. Horowitz LF, Hirdes W, Suh BC, Hilgemann DW, Mackie K, Hille B: Phospholipase C in living cells: activation, inhibition, Ca2+ requirement, and regulation of M current. J Gen Physiol 2005;126:243-262
37. Hildebrandt JP, Plant TD, Meves H: The effects of bradykinin on K+ currents in NG108-15 cells treated with U73122, a phospholipase C inhibitor, or neomycin. Br J Pharmacol 1997;120:841-850
38. Namkoong S, Kim CK, Cho YL, Kim JH, Lee H, Ha KS, Choe J, Kim PH, Won MH, Kwon YG, Shim EB, Kim YM: Forskolin increases angiogenesis through the coordinated cross-talk of PKA-dependent VEGF expression and Epac-mediated PI3K/Akt/eNOS signaling. Cell Signal 2009;21:906-915
39. Tang Z, Shi D, Jia B, Chen J, Zong C, Shen D, Zheng Q, Wang J, Tong X: Exchange protein activated by cyclic adenosine monophosphate regulates the switch between adipogenesis and osteogenesis of human mesenchymal stem cells through increasing the activation of phosphatidylinositol 3-kinase. Int J Biochem Cell Biol 2012;44:1106-1120
40. Kashima Y, Miki T, Shibasaki T, Ozaki N, Miyazaki M, Yano H, Seino S: Critical role of cAMP-GEFII--Rim2 complex in incretin-potentiated insulin secretion. J Biol Chem 2001;276:46046-46053
41. Renstrom E, Eliasson L, Rorsman P: Protein kinase A-dependent and -independent stimulation of exocytosis by cAMP in mouse pancreatic B-cells. J Physiol 1997;502 (Pt 1):105-118
42. Weber S, Zeller M, Guan K, Wunder F, Wagner M, El-Armouche A: PDE2 at the crossway between cAMP and cGMP signalling in the heart. Cell Signal 2017;38:76-84
43. Pelligrino DA, Wang Q: Cyclic nucleotide crosstalk and the regulation of cerebral vasodilation. Prog Neurobiol 1998;56:1-18
44. Corbin JD, Turko IV, Beasley A, Francis SH: Phosphorylation of phosphodiesterase-5 by cyclic nucleotide-dependent protein kinase alters its catalytic and allosteric cGMP-binding activities. Eur J Biochem 2000;267:2760-2767
45. Murthy KS: Activation of phosphodiesterase 5 and inhibition of guanylate cyclase by cGMP-dependent protein kinase in smooth muscle. Biochem J 2001;360:199-208
46. Undank S, Kaiser J, Sikimic J, Düfer M, Krippeit-Drews P, Drews G: Atrial natriuretic peptide affects stimulus-secretion coupling of pancreatic beta-cells. Diabetes 2017;66:2840-2848
47. Gromada J, Bokvist K, Ding WG, Barg S, Buschard K, Renstrom E, Rorsman P: Adrenaline stimulates glucagon secretion in pancreatic A-cells by increasing the Ca2+ current and the number of granules close to the L-type Ca2+ channels. J Gen Physiol 1997;110:217-228
48. Skelin M, Rupnik M: cAMP increases the sensitivity of exocytosis to Ca(2)+ primarily through protein kinase A in mouse pancreatic beta cells. Cell Calcium 2011;49:89-99
49. Kasai H, Suzuki T, Liu TT, Kishimoto T, Takahashi N: Fast and cAMP-sensitive mode of Ca(2+)-dependent exocytosis in pancreatic beta-cells. Diabetes 2002;51 Suppl 1:S19-24

Figure legends

Fig. 1 OLA increases $[Ca^{2+}]_c$ of mouse and human beta-cells. A) Representative measurement showing enhancement of glucose-induced oscillations of $[Ca^{2+}]_c$ in a mouse beta-cell by OLA (1 μM) in the presence of 15 mM glucose. B) Summary of all experiments of this series. C,D) Effect of OLA (10 μM) in the presence of 15 mM glucose. E) Representative experiment showing the effect of 1 μM OLA on a human beta-cell in the presence of 10 mM glucose. F) Summary of all experiments of this series. The number in the columns indicates the number of experiments with different cell clusters from 3-4 mice. Experiments with human beta-cells were performed with dispersed islets from one organ donor. *P ≤ 0.05, ***P ≤ 0.001.

Fig. 2 OLA stimulates insulin secretion in mouse islets. A) Averaged curve showing the stimulating effect of OLA on insulin secretion in perifusion experiments. OLA (1 μM) was applied during the 2nd phase of insulin secretion. B) Mean insulin secretion rate was analyzed for 10 min before and after adding OLA in the 2nd phase of insulin secretion. C) To evaluate the effect on the 1st phase of insulin secretion, OLA (1 μM) was added before the increase of the glucose concentration. Averaged curves with OLA (solid line) and without OLA (dashed line) showing the 1st phase of insulin secretion. D) Mean insulin secretion rate during the first 15 min of the 1st phase of insulin secretion in the presence of 15 mM glucose with and without OLA was analyzed. E) Steady-state glucose-induced insulin secretion measured for 1 hour is enhanced by 1 and 10 μM OLA but not by 0.1 μM. F) Glucose-dependency of the effect of OLA (1 μM) on steady-state insulin secretion. The number in the columns indicates the number of experiments with islets from 6-13 mice. *P≤ 0.05, **P ≤ 0.01, ***P ≤ 0.001.

Fig. 3 A $G_{\alpha s}$-coupled receptor but not FXR is the target of OLA. A) Representative trace showing the effect of OLA (1 μM) in the presence of 15 mM glucose on a beta-cell of a $FXR^{-/-}$ mouse. B) Summary of all experiments of this series. C) Steady-state glucose-induced insulin secretion from islets of $FXR^{-/-}$ mice is enhanced by OLA (1 μM). D) Inhibition of $G_{\alpha s}$

by NF449 (10 μM) prevents the stimulating effect of OLA (1 μM) on insulin secretion in islets from WT mice. The number in the columns indicates the number of experiments with different cell clusters or islets from 4-6 mice. **P ≤ 0.01, ***P ≤ 0.001.

Fig. 4 Different TGR5 agonists mimic stimulating effects on $[Ca^{2+}]_c$ and insulin secretion in beta-cells. A) Representative measurement showing enhancement of glucose-induced oscillations of $[Ca^{2+}]_c$ by RG239 (1 μM) in the presence of 15 mM glucose. B) Summary of all experiments of this series. C) Steady-state glucose-induced insulin secretion is stimulated by RG239 compared to control islets. D) Representative measurement showing the stimulating effect on glucose-induced oscillations of $[Ca^{2+}]_c$ by TUDCA (50 μM) in the presence of 15 mM glucose. E) Summary of all experiments of this series. F) Steady-state glucose-induced insulin secretion is increased by TUDCA. The number in the columns indicates the number of experiments with different cell clusters or islets from 3-6 mice. *P ≤ 0.05, ***P ≤ 0.001.

Fig. 5 OLA acutely affects K_{ATP} and Ca^{2+} currents of mouse beta-cells. A) Representative experiment showing K_{ATP} current measured in the perforated-patch configuration of the patch-clamp technique. Administration of OLA (1 μM) leads to reduction of K_{ATP} current in the presence of 0.5 mM glucose. The current is identified as K_{ATP} current by the specific K_{ATP} channel opener diazoxide (250 μM). B) Summary of all experiments of this series, normalized to the current under control condition. C,D) Increased concentration of OLA (10 μM) amplifies the reduction of the K_{ATP} current. E) Currents through voltage-dependent Ca^{2+} channels were measured in the perforated-patch configuration. The representative measurement shows an enhancement of the maximal Ca^{2+} current during OLA administration compared to control condition in the presence of 15 mM glucose. F) Summary of all experiments of this series at different time points of OLA application, normalized to the

current under control condition. The number in the columns indicates the number of experiments with different cell clusters from 3-4 mice. ***P ≤ 0.001.

Fig. 6 OLA (10 μM) induces a biphasic effect on Ca^{2+} currents and insulin secretion and depolarized V_m. A) Currents through voltage-dependent Ca^{2+} channels were measured in the perforated-patch configuration. The representative measurement shows an enhancement of the maximal Ca^{2+} current after 2 min of OLA administration (10 μM) compared to control condition in the presence of 15 mM glucose. Eight min of OLA application clearly reduced the current. B) Summary of all experiments of this series at different time points of OLA application, normalized to the current under control condition. C) Averaged curve showing the transient stimulating effect of 10 μM OLA on the 2^{nd} phase of insulin secretion in perifusion experiments. D) Mean insulin secretion rate was analyzed at the time intervals indicated by the symbols. ★ 10 min before OLA application; ▲ 5 min after OLA application; ▼ 10 min before wash-out

OLA-evoked changes in V_m were suppressed by PKA inhibition. E) Representative experiment showing that OLA (10 μM) depolarized V_m and increased action potential frequency. F) Summary of the results concerning the plateau potential. G) Summary of the results concerning spike frequency. H) Representative experiment in the presence of KT5720 (5 μM) showing that the inhibitor suppresses the OLA effect. I,K) Summary of the results of this series. The number in the columns indicates the number of experiments with different cell clusters or islets from 4-6 mice. *P ≤ 0.05, **P ≤ 0.01, ***P ≤ 0.001.

Fig. 7 Inhibition of the AC but not the knockout of Epac2 prevents the effect of OLA. A) Inhibition of the AC with DDA (100 μM) prevents the stimulatory effect of OLA (1 μM) on insulin secretion of islets from WT mice. B) OLA (1 μM) increases the intracellular cAMP concentration in islets from WT mice in the presence of 15 mM glucose. C) Effect of OLA (1 μM) on $[Ca^{2+}]_c$ in the presence of 15 mM glucose in beta-cells from $Epac2^{-/-}$ mice. D) In islets

of Epac2$^{-/-}$ mice, steady-state glucose-induced insulin secretion is increased by OLA (1 μM) and RG239 (1 μM) compared to control islets. The number in the columns indicates the number of experiments with different cell clusters or islets from 3-6 mice. *P ≤ 0.05, **P ≤ 0.01, ***P ≤ 0.001.

Fig. 8 Stimulating effects of OLA on insulin secretion are mediated by PKA but not by PLC or PI3K. Experiments were performed with islets from WT mice. A) The PKA antagonist Myr-PKI (1 μM) eliminates the increasing effect of OLA. B) Another PKA antagonist, KT5720 (5 μM), also prevents the stimulation by OLA. C) The PLC antagonist edelfosine (10 μM) does not influence the effect of OLA. D) The PI3K inhibitor wortmannin (100 nM) does not reduce the stimulation by OLA. The number in the columns indicates the number of experiments with different islets from 6 mice. *P ≤ 0.05, **P ≤ 0.01, ***P ≤ 0.001.

Fig. 9 The stimulating effect of OLA on beta-cells is not mediated by GLP-1 from alpha-cells. A) Inhibition of the GLP-1 receptor by the antagonist exendin 9-39 (100 nM) in WT islets does not influence the OLA-mediated increase of insulin secretion. B) The potency of exendin 9-39 (100 nM) to inhibit the GLP-1 receptor is demonstrated by the abolishment of the GLP-1-induced (50 nM) increase in insulin secretion. C) In MIN6 cells, glucose-induced insulin secretion (15 mM glucose) is increased by OLA. The number in the columns indicates the number of experiments. Islets for the series with exendin 9-39 were from 7 different mice. *P ≤ 0.05, **P ≤ 0.01, ***P ≤ 0.001.

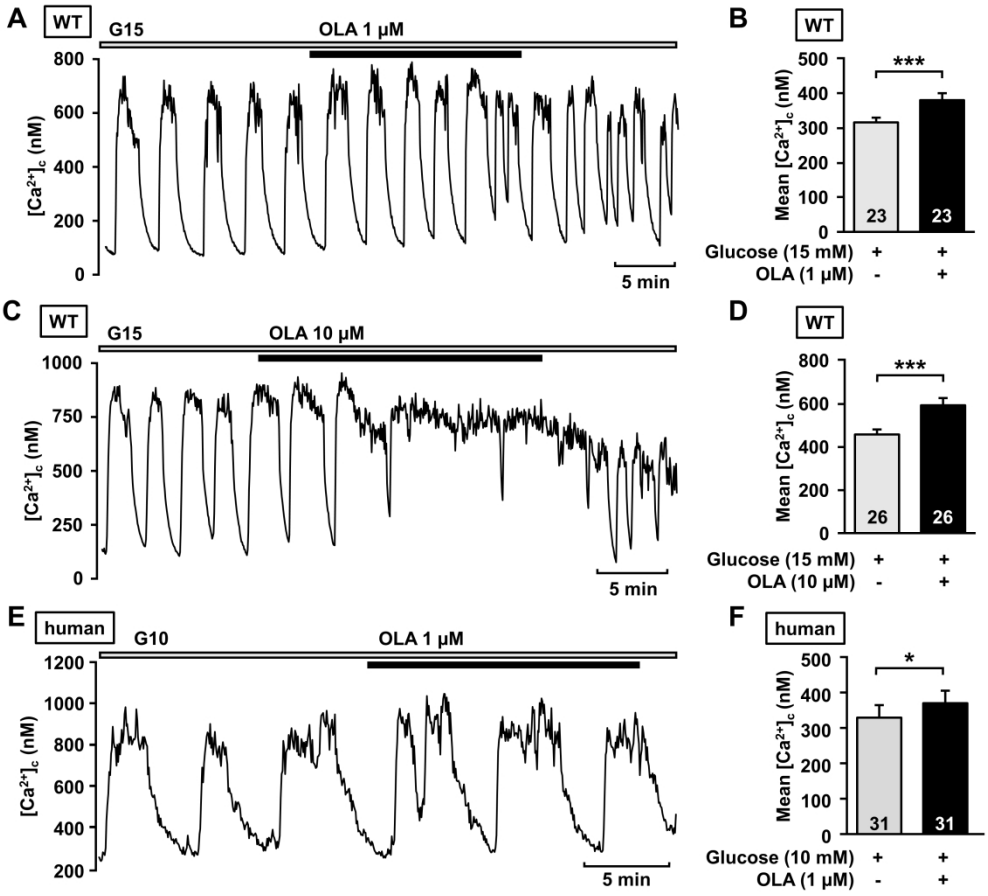

Fig. 1 OLA increases [Ca2+]c of mouse and human beta-cells. A) Representative measurement showing enhancement of glucose-induced oscillations of [Ca2+]c in a mouse beta-cell by OLA (1 µM) in the presence of 15 mM glucose. B) Summary of all experiments of this series. C,D) Effect of OLA (10 µM) in the presence of 15 mM glucose. E) Representative experiment showing the effect of 1 µM OLA on a human beta-cell in the presence of 10 mM glucose. F) Summary of all experiments of this series. The number in the columns indicates the number of experiments with different cell clusters from 3-4 mice. Experiments with human beta-cells were performed with dispersed islets from one organ donor. *P ≤ 0.05, ***P ≤ 0.001.

305x279mm (300 x 300 DPI)

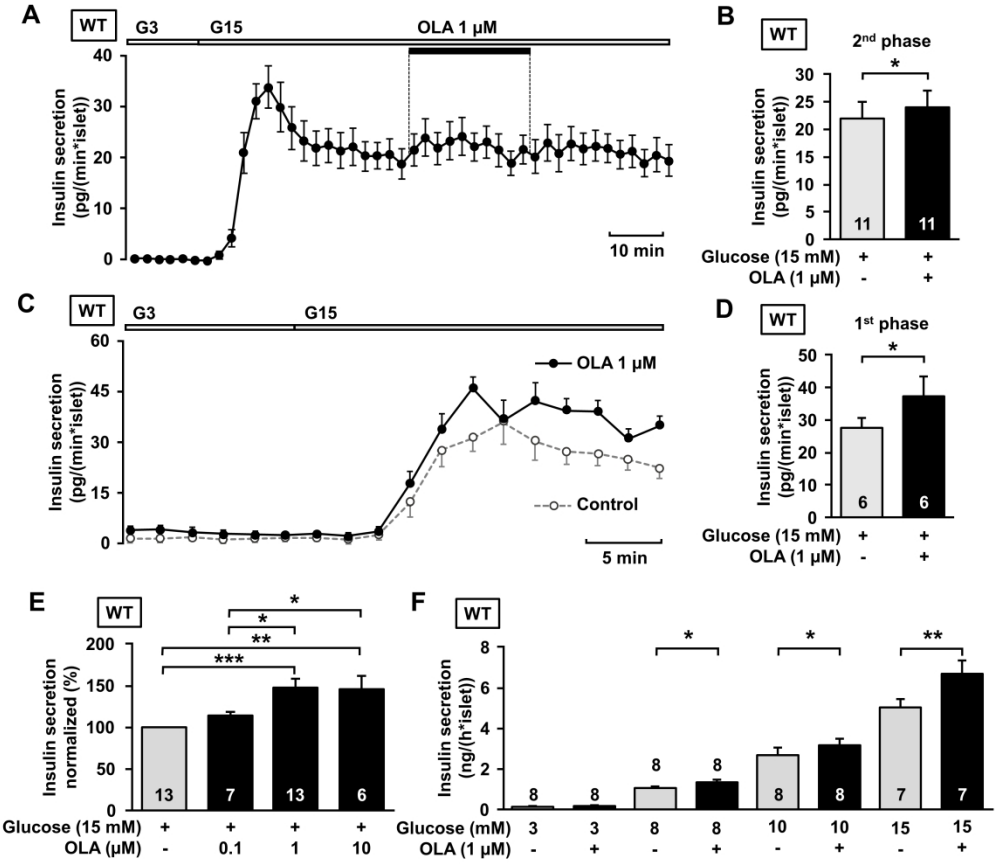

Fig. 2 OLA stimulates insulin secretion in mouse islets. A) Averaged curve showing the stimulating effect of OLA on insulin secretion in perifusion experiments. OLA (1 µM) was applied during the 2nd phase of insulin secretion. B) Mean insulin secretion rate was analyzed for 10 min before and after adding OLA in the 2nd phase of insulin secretion. C) To evaluate the effect on the 1st phase of insulin secretion, OLA (1 µM) was added before the increase of the glucose concentration. Averaged curves with OLA (solid line) and without OLA (dashed line) showing the 1st phase of insulin secretion. D) Mean insulin secretion rate during the first 15 min of the 1st phase of insulin secretion in the presence of 15 mM glucose with and without OLA was analyzed. E) Steady-state glucose-induced insulin secretion measured for 1 hour is enhanced by 1 and 10 µM OLA but not by 0.1 µM. F) Glucose-dependency of the effect of OLA (1 µM) on steady-state insulin secretion. The number in the columns indicates the number of experiments with islets from 6-13 mice. *P≤ 0.05, **P ≤ 0.01, ***P ≤ 0.001.

325x286mm (300 x 300 DPI)

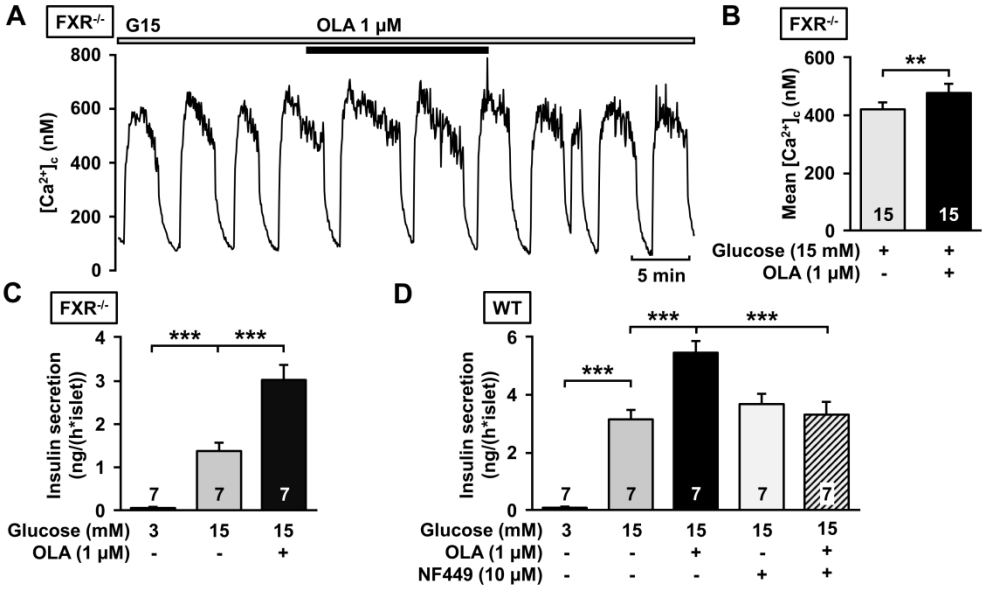

Fig. 3 A Gαs-coupled receptor but not FXR is the target of OLA. A) Representative trace showing the effect of OLA (1 µM) in the presence of 15 mM glucose on a beta-cell of a FXR /- mouse. B) Summary of all experiments of this series. C) Steady-state glucose-induced insulin secretion from islets of FXR-/- mice is enhanced by OLA (1 µM). D) Inhibition of Gαs by NF449 (10 µM) prevents the stimulating effect of OLA (1 µM) on insulin secretion in islets from WT mice. The number in the columns indicates the number of experiments with different cell clusters or islets from 4-6 mice. **P ≤ 0.01, ***P ≤ 0.001.

305x184mm (300 x 300 DPI)

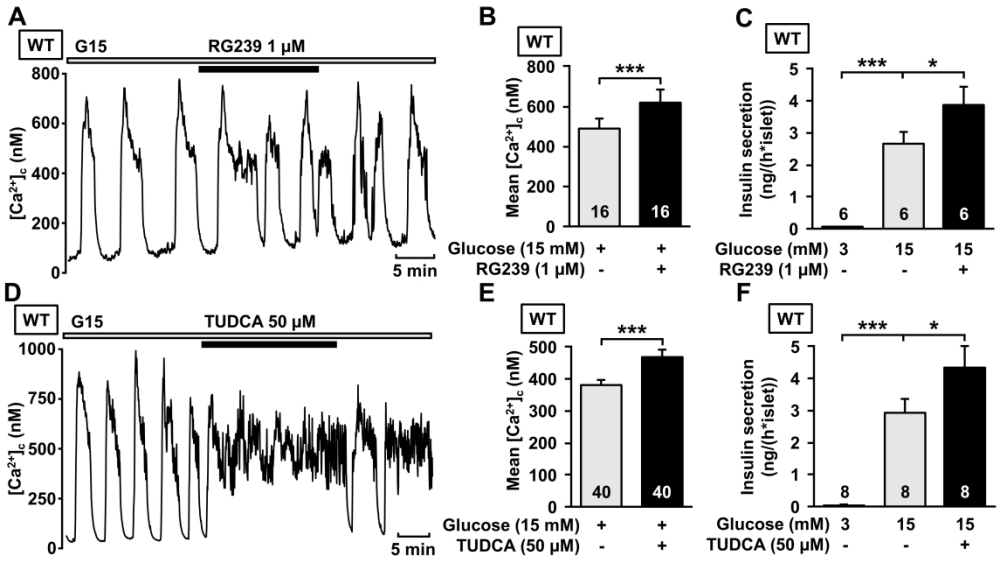

Fig. 4 Different TGR5 agonists mimic stimulating effects on [Ca2+]c and insulin secretion in beta-cells. A) Representative measurement showing enhancement of glucose-induced oscillations of [Ca2+]c by RG239 (1 µM) in the presence of 15 mM glucose. B) Summary of all experiments of this series. C) Steady-state glucose-induced insulin secretion is stimulated by RG239 compared to control islets. D) Representative measurement showing the stimulating effect on glucose-induced oscillations of [Ca2+]c by TUDCA (50 µM) in the presence of 15 mM glucose. E) Summary of all experiments of this series. F) Steady-state glucose-induced insulin secretion is increased by TUDCA. The number in the columns indicates the number of experiments with different cell clusters or islets from 3-6 mice. *P ≤ 0.05, ***P ≤ 0.001.

329x184mm (300 x 300 DPI)

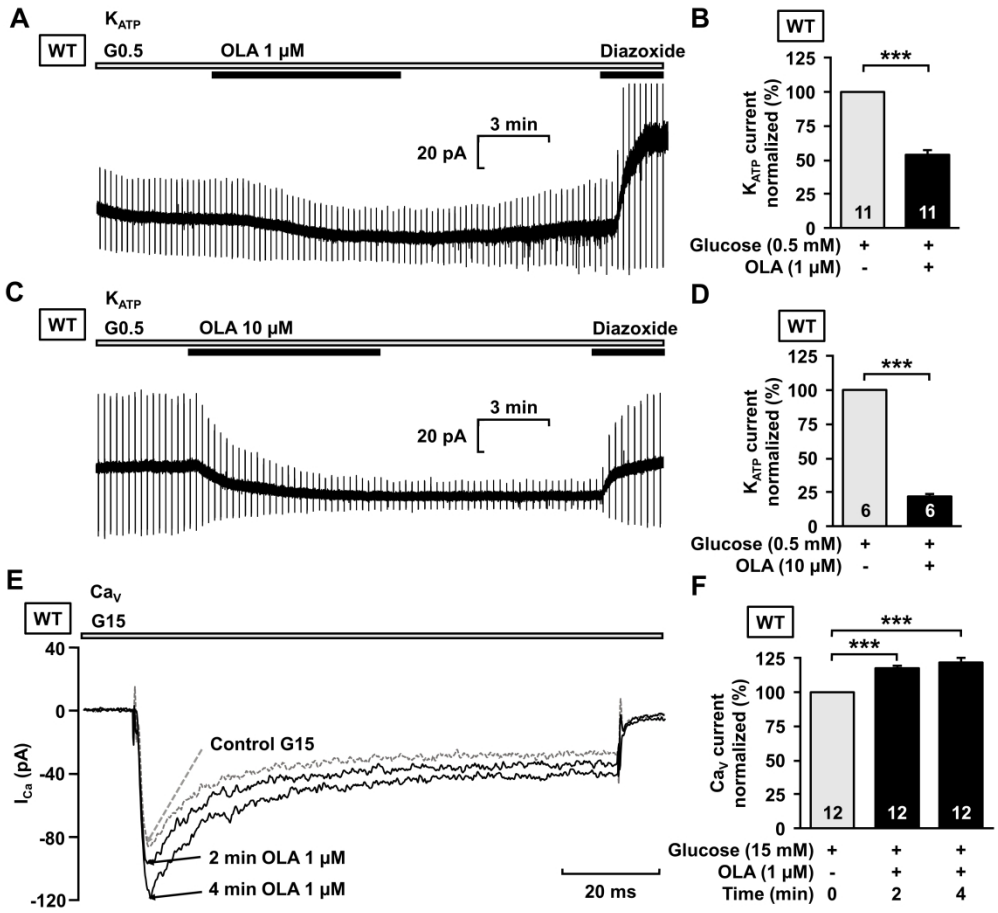

Fig. 5 OLA acutely affects KATP and Ca2+ currents of mouse beta-cells. A) Representative experiment showing KATP current measured in the perforated-patch configuration of the patch-clamp technique. Administration of OLA (1 µM) leads to reduction of KATP current in the presence of 0.5 mM glucose. The current is identified as KATP current by the specific KATP channel opener diazoxide (250 µM). B) Summary of all experiments of this series, normalized to the current under control condition. C,D) Increased concentration of OLA (10 µM) amplifies the reduction of the KATP current. E) Currents through voltage-dependent Ca2+ channels were measured in the perforated-patch configuration. The representative measurement shows an enhancement of the maximal Ca2+ current during OLA administration compared to control condition in the presence of 15 mM glucose. F) Summary of all experiments of this series at different time points of OLA application, normalized to the current under control condition. The number in the columns indicates the number of experiments with different cell clusters from 3-4 mice. ***P ≤ 0.001.

309x283mm (300 x 300 DPI)

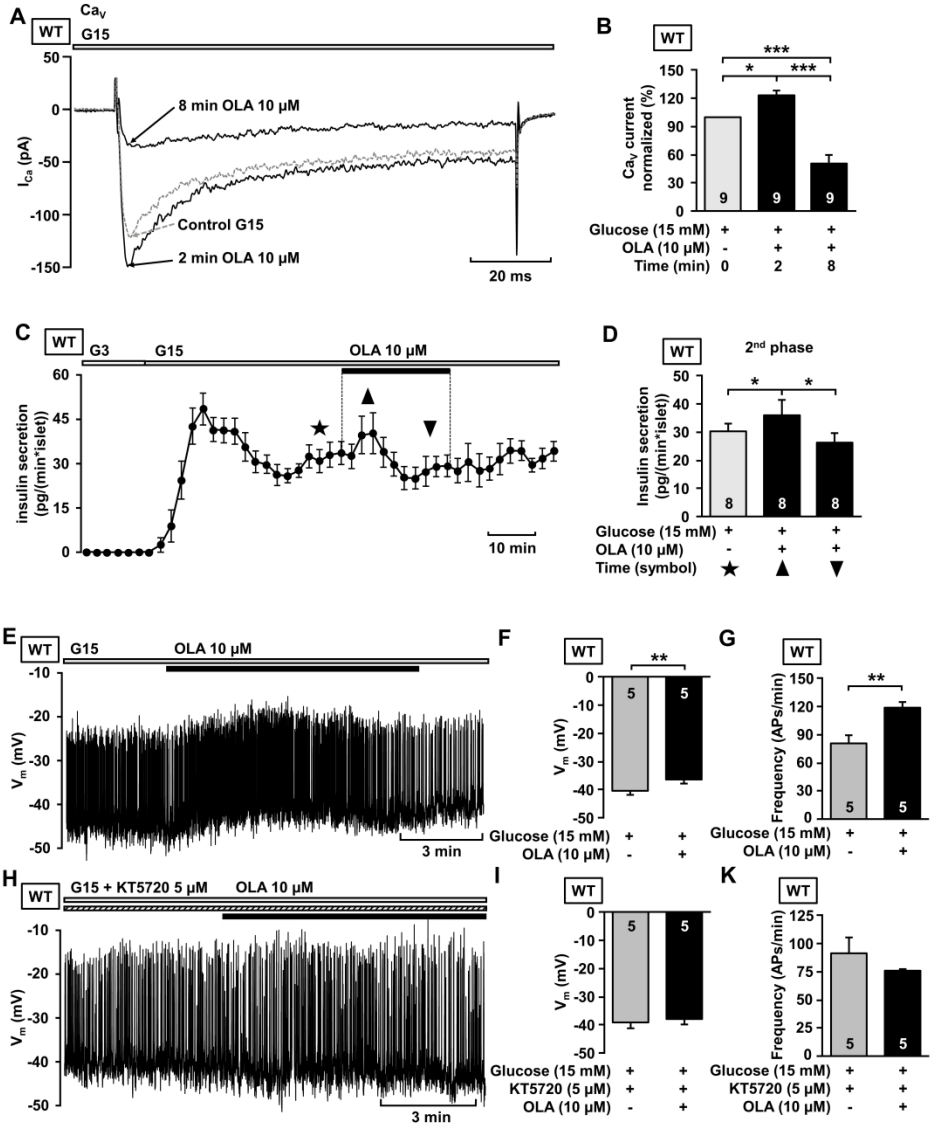

Fig. 6 OLA (10 µM) induces a biphasic effect on Ca2+ currents and insulin secretion and depolarized Vm. A) Currents through voltage-dependent Ca2+ channels were measured in the perforated-patch configuration. The representative measurement shows an enhancement of the maximal Ca2+ current after 2 min of OLA administration (10 µM) compared to control condition in the presence of 15 mM glucose. Eight min of OLA application clearly reduced the current. B) Summary of all experiments of this series at different time points of OLA application, normalized to the current under control condition. C) Averaged curve showing the transient stimulating effect of 10 µM OLA on the 2nd phase of insulin secretion in perifusion experiments. D) Mean insulin secretion rate was analyzed at the time intervals indicated by the symbols. ★ 10 min before OLA application; ▲ 5 min after OLA application; ▼ 10 min before wash-out OLA-evoked changes in Vm were suppressed by PKA inhibition. E) Representative experiment showing that OLA (10 µM) depolarized Vm and increased action potential frequency. F) Summary of the results concerning the plateau potential. G) Summary of the results concerning spike frequency. H) Representative experiment in the presence of KT5720 (5 µM) showing that the inhibitor suppresses the OLA effect. I,K) Summary of the results of this series. The number in the columns indicates the number of experiments with different cell clusters or islets

from 4-6 mice. *P ≤ 0.05, **P ≤ 0.01, ***P ≤ 0.001.

360x450mm (300 x 300 DPI)

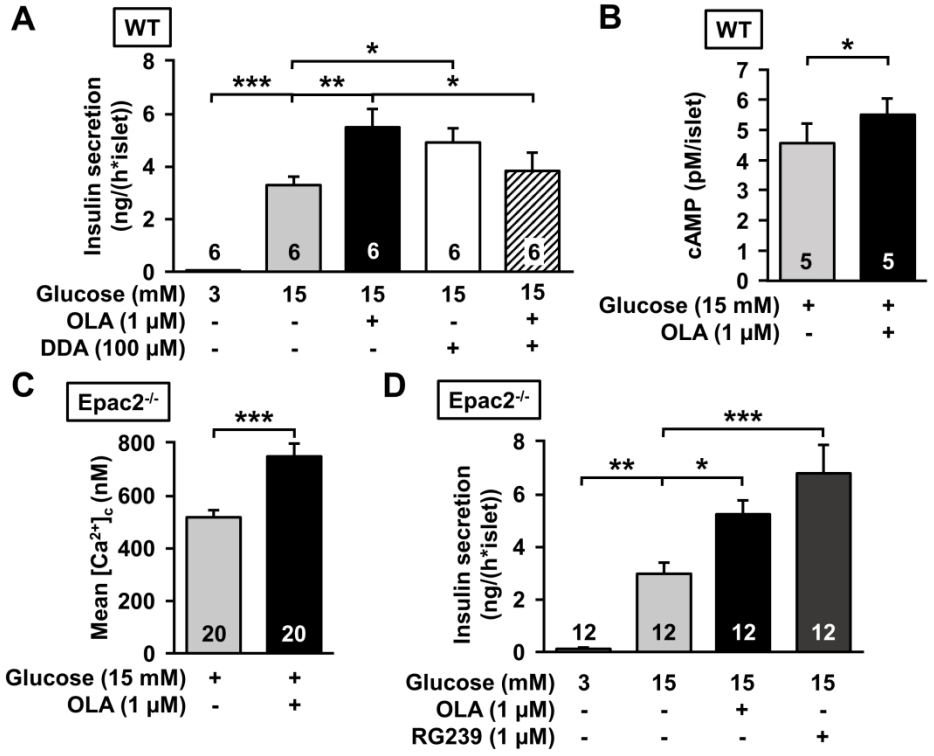

Fig. 7 Inhibition of the AC but not the knockout of Epac2 prevents the effect of OLA. A) Inhibition of the AC with DDA (100 µM) prevents the stimulatory effect of OLA (1 µM) on insulin secretion of islets from WT mice. B) OLA (1 µM) increases the intracellular cAMP concentration in islets from WT mice in the presence of 15 mM glucose. C) Effect of OLA (1 µM) on [Ca2+]c in the presence of 15 mM glucose in beta-cells from Epac2-/- mice. D) In islets of Epac2-/- mice, steady-state glucose-induced insulin secretion is increased by OLA (1 µM) and RG239 (1 µM) compared to control islets. The number in the columns indicates the number of experiments with different cell clusters or islets from 3-6 mice. *P ≤ 0.05, **P ≤ 0.01, ***P ≤ 0.001.

250x199mm (300 x 300 DPI)

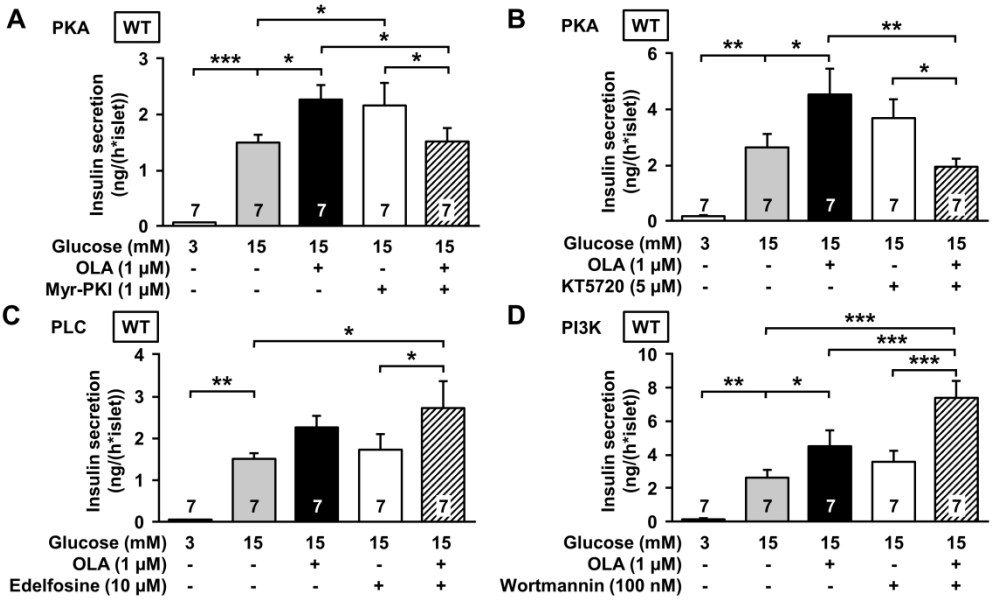

Fig. 8 Stimulating effects of OLA on insulin secretion are mediated by PKA but not by PLC or PI3K. Experiments were performed with islets from WT mice. A) The PKA antagonist Myr-PKI (1 µM) eliminates the increasing effect of OLA. B) Another PKA antagonist, KT5720 (5 µM), also prevents the stimulation by OLA. C) The PLC antagonist edelfosine (10 µM) does not influence the effect of OLA. D) The PI3K inhibitor wortmannin (100 nM) does not reduce the stimulation by OLA. The number in the columns indicates the number of experiments with different islets from 6 mice. *P ≤ 0.05, **P ≤ 0.01, ***P ≤ 0.001.

314x189mm (300 x 300 DPI)

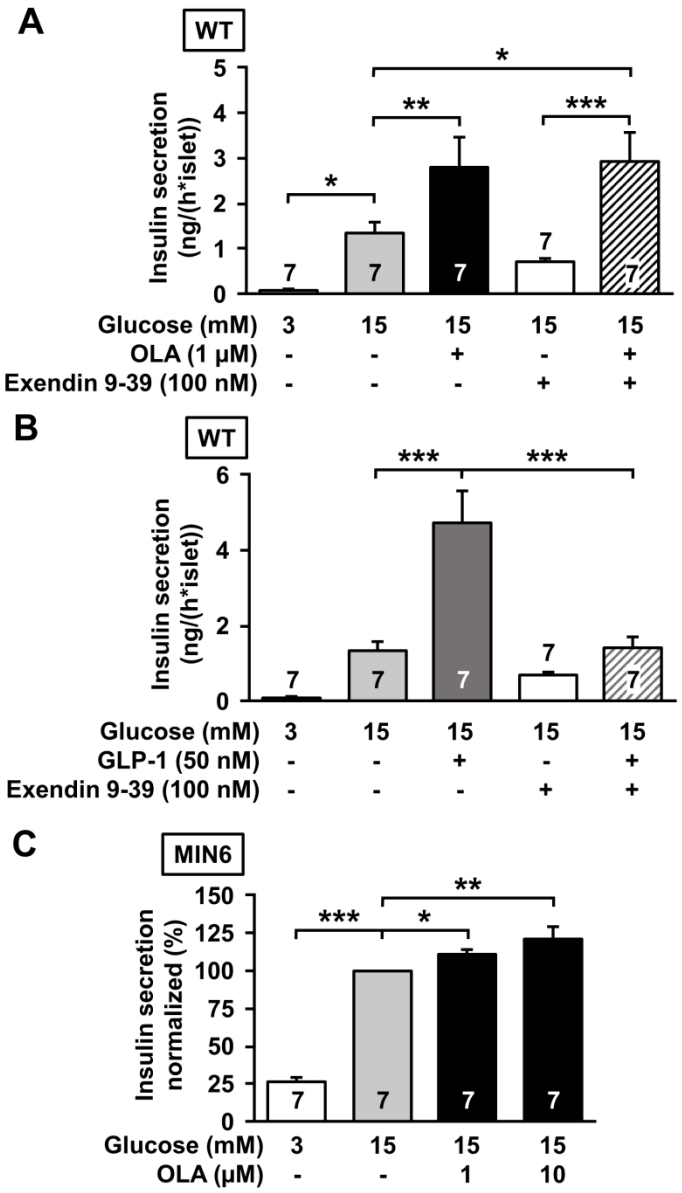

Fig. 9 The stimulating effect of OLA on beta-cells is not mediated by GLP-1 from alpha-cells. A) Inhibition of the GLP-1 receptor by the antagonist exendin 9-39 (100 nM) in WT islets does not influence the OLA-mediated increase of insulin secretion. B) The potency of exendin 9-39 (100 nM) to inhibit the GLP-1 receptor is demonstrated by the abolishment of the GLP-1-induced (50 nM) increase in insulin secretion. C) In MIN6 cells, glucose-induced insulin secretion (15 mM glucose) is increased by OLA. The number in the columns indicates the number of experiments. Islets for the series with exendin 9-39 were from 7 different mice. *P ≤ 0.05, **P ≤ 0.01, ***P ≤ 0.001.

160x279mm (300 x 300 DPI)